

# Synthesis of Molybdenum Nitrido Complexes for Triple-Bond Metathesis of Alkynes and Nitriles

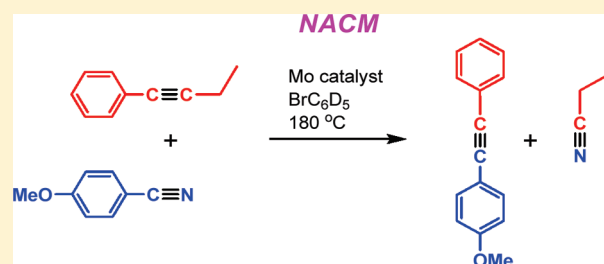
Eric S. Wiedner,<sup>†,§</sup> Kimberley J. Gallagher,<sup>‡</sup> Marc J. A. Johnson,<sup>\*,‡</sup> and Jeff W. Kampf<sup>†</sup>

<sup>†</sup>Department of Chemistry, University of Michigan, 930 North University Avenue, Ann Arbor, Michigan 48109-1055, United States

<sup>‡</sup>Chemical Sciences and Engineering Division, Argonne National Laboratory, Argonne, Illinois 60439, United States

**S** Supporting Information

**ABSTRACT:** Complexes of the type  $N\equiv Mo(OR)_3$  ( $R$  = tertiary alkyl, tertiary silyl, bulky aryl) have been synthesized in the search for molybdenum-based nitrile–alkyne cross-metathesis (NACM) catalysts. Protonolysis of known  $N\equiv Mo(NMe_2)_3$  led to the formation of  $N\equiv Mo(O-2,6-^iPr_2C_6H_3)_3(NHMe_2)$  (**12**),  $N\equiv Mo(OSiPh_3)_3(NHMe_2)$  (**5-NHMe<sub>2</sub>**), and  $N\equiv Mo(OCPh_2Me)_3(NHMe_2)$  (**17-NHMe<sub>2</sub>**). The X-ray structure of **12** revealed an  $NHMe_2$  ligand bound *cis* to the nitrido ligand, while **5-NHMe<sub>2</sub>** possessed an  $NHMe_2$  bound *trans* to the nitride ligand. Consequently, **17-NHMe<sub>2</sub>** readily lost its amine ligand to form  $N\equiv Mo(OCPh_2Me)_3$  (**17**), while **12** and **5-NHMe<sub>2</sub>** retained their amine ligands in solution. Starting from bulkier tris-anilide complexes,  $N\equiv Mo(N[R]Ar)_3$  ( $R$  = isopropyl, *tert*-butyl;  $Ar$  = 3,5-dimethylphenyl) allowed for the formation of base-free complexes  $N\equiv Mo(OSiPh_3)_3$  (**5**) and  $N\equiv Mo(OSiPh_2^tBu)_3$  (**16**). Achievement of a NACM cycle requires the nitride complex to react with alkynes to form alkylidyne complexes; therefore the alkyne cross-metathesis (ACM) activity of the complexes was tested. Complex **5** was found to be an efficient catalyst for the ACM of 1-phenyl-1-butyne at room temperature. Complexes **12** and **5-NHMe<sub>2</sub>** were also active for ACM at 75 °C, while **17-NHMe<sub>2</sub>** and **16** did not show ACM activity. Only **5** proved to be active for the NACM of anisonitrile, which is a reactive substrate in NACM catalyzed by tungsten. NACM with **5** required a reaction temperature of 180 °C in order to initiate the requisite alkylidyne-to-nitride conversion, with slightly more than two turnovers achieved prior to catalyst deactivation. Known molybdenum nitrido complexes were screened for NACM activity under similar conditions, and only  $N\equiv Mo(OSiPh_3)_3(py)$  (**5-py**) displayed any trace of NACM activity.



## INTRODUCTION

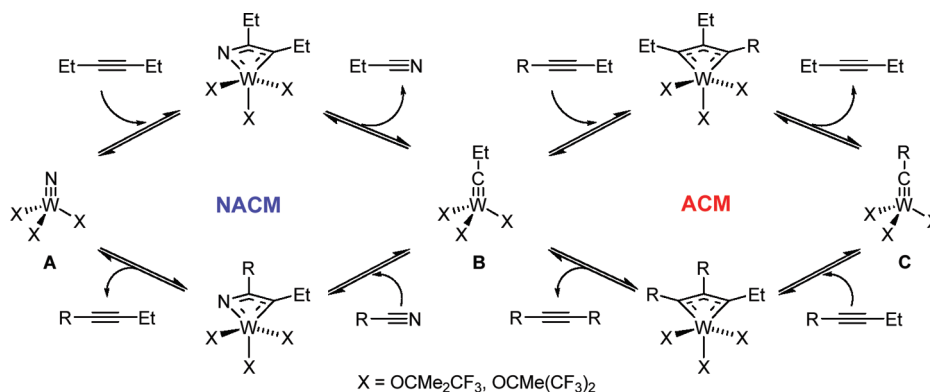
The formation of carbon–carbon bonds is a key challenge in the construction of complex molecules. The development of highly active olefin and alkyne metathesis catalysts has led to great advances in organic and polymer synthesis.<sup>1–4</sup> During the past decade, alkyne cross-metathesis (ACM) has emerged as a valuable tool in the synthesis of a variety of molecular structures. Poly(arylene-ethynylene) chains, which often display useful optical properties, have been synthesized via ACM<sup>3</sup> without many of the structural ambiguities that arise when Pd-catalyzed cross-coupling is employed.<sup>5</sup> Related arylene-ethynylene macrocyclic structures of various ring sizes can often be synthesized via ACM in higher yields than obtainable with Pd-catalyzed cross-coupling.<sup>4</sup> For example, a carbazole-derived arylene-ethynylene tetramer that was synthesized through ACM was shown to detect explosives via fluorescence quenching.<sup>6</sup> In addition, the synthesis of biologically relevant molecules can be facilitated by ACM, as demonstrated in the synthesis of epothilone C, a member of a family of chemotherapy drugs.<sup>7</sup> A key sequence in the epothilone C synthesis was the formation of a complex cyclic ring system through ACM, followed by reduction of the alkyne fragment into a Z-alkene via a Lindlar reduction.<sup>7</sup>

The nitrile functionality can frequently be incorporated into a molecule more readily than the alkyne moiety.<sup>8</sup> As an alternative to ACM, we reported nitrile-alkyne cross-metathesis (NACM) in which symmetrical alkynes (RCCR) can be synthesized via the catalytic cross-metathesis of a nitrile substrate (RCN) and 3-hexyne (EtCCet).<sup>9,10</sup> The NACM reaction is catalyzed by the tungsten nitride complexes  $N\equiv W(OCMe(CF_3)_2)_3(DME)$  (**1**) and  $[N\equiv W(OCMe_2CF_3)_3]_3$  (**2**). In the catalytic cycle (Scheme 1, left side), the nitride complex (**A**) first reacts with EtCCet to generate an alkylidyne complex (**B**) and propionitrile (EtCN) through an intermediate azametalcyclobutadiene complex. The NACM cycle is completed via reaction of **B** with RCN to return **A** with the concurrent formation of RCCet. Mechanistic studies revealed that **B** is more active for ACM than NACM, and so RCCR is formed primarily through an overlapping ACM cycle (Scheme 1, right side).<sup>10</sup> Despite being slower than ACM, NACM is required for the initial introduction of RC fragments into the alkyne products. The utility of NACM has been demonstrated in the synthesis of the aforementioned

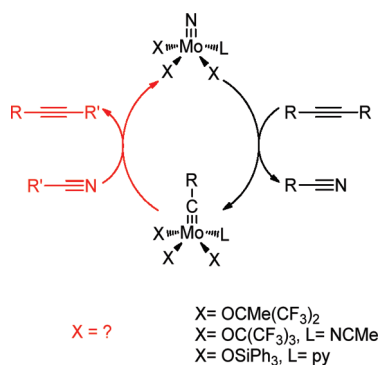
Received: December 4, 2010

Published: June 01, 2011

Scheme 1. NACM via Reversible Interconversion of Nitride and Alkyldiyne Ligands



Scheme 2. Interconversions of Mo Nitride and Alkyldiyne Complexes



carbazole-derived arylene-ethynylene tetramer, which was formed in fewer steps than previously achieved with ACM.<sup>10,4d</sup>

We desired to discover whether NACM could be achieved with any metal other than tungsten. In order to catalyze NACM, the metal complex must be able to reversibly interconvert between nitride and alkyldiyne ligands through an azametacyclobutadiene intermediate or transition state.<sup>10</sup> Molybdenum seemed the most likely candidate due to the similarity of molybdenum and tungsten ACM catalysts. In 2006, our group reported the first examples of a molybdenum nitride-to-alkyldiyne conversion, starting from  $\text{N}\equiv\text{Mo}(\text{OCMe}(\text{CF}_3)_2)_3$  (**3**) and  $\text{N}\equiv\text{Mo}(\text{OC}(\text{CF}_3)_3)_3(\text{NCMe})$  (**4**) (Scheme 2, right pathway), which both serve as ACM catalysts.<sup>11</sup> Complex **3** was stoichiometrically converted into its propylidyne analogue  $\text{EtC}\equiv\text{Mo}(\text{OCMe}(\text{CF}_3)_2)_3$ , which was isolated and characterized. During the course of the present work, Fürstner et al. reported that the complex  $\text{N}\equiv\text{Mo}(\text{OSiPh}_3)_3(\text{py})$  (**5-py**) is also an active ACM catalyst precursor.<sup>12</sup> However, the reverse alkyldiyne-to-nitride conversion has never been observed for a molybdenum complex (Scheme 2, left pathway). In accordance with this fact, neither **3** nor **4** catalyzes NACM,<sup>13,14</sup> while the NACM activity of **5-py** and its benzylidyne analog<sup>15</sup> were not reported.

The inability of **3** or **4** to catalyze NACM likely stems from two inherent differences between molybdenum and tungsten. First, molybdenum complexes possess a larger barrier for metalacycle formation than analogous tungsten complexes. This is observed experimentally in the slower rates of ACM for molybdenum alkyldiyne complexes relative to their tungsten counterparts.<sup>16</sup>

Additionally, the difference in activation barriers is underscored by the fact that tungsten metalacyclobutadiene complexes are often stable enough to be isolated,<sup>17</sup> but molybdenum metalacyclobutadiene complexes are rarely observable even at low temperatures.<sup>18</sup> Theoretical investigations have attributed this trend to the diminished spatial extension of the molybdenum 4d orbitals relative to the tungsten 5d orbitals, which leads to an intrinsically larger barrier for metalacycle formation with molybdenum complexes.<sup>19</sup> For a given metal, the barrier to metalacycle formation can be lowered by decreasing the electron-donor ability of the ancillary ligands, which increases the Lewis acidity of the metal.<sup>19</sup> Experiments confirm this trend, as electron-deficient  $\text{Me}_3\text{CC}\equiv\text{Mo}(\text{OCMe}(\text{CF}_3)_2)_3$  metathesizes alkynes more rapidly than its  $-\text{OCMe}_2\text{CF}_3$  and  $-\text{OCMe}_3$  congeners.<sup>20</sup> In the case of tungsten, the effect can be so dramatic that expulsion of the alkyne from the metalacyclobutadiene complex becomes rate-determining,<sup>17a</sup> and evidence for the associative exchange of alkyne at the metalacyclobutadiene is observed in an extreme case.<sup>17b</sup> An exactly analogous effect is found in degenerate nitrogen atom exchange.<sup>21,22</sup> Therefore, it is expected that molybdenum NACM catalysts will require relatively weak electron-donor ligands in order to allow azametacycle formation to be energetically accessible.

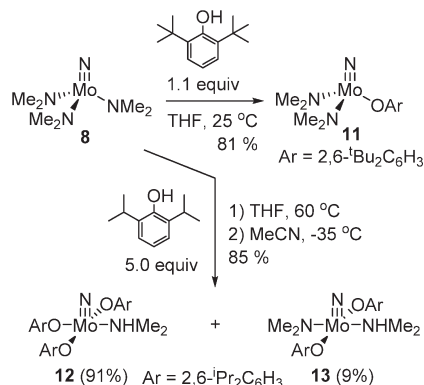
In an ideal NACM catalyst, the nitride and alkyldiyne forms of the catalyst would be nearly isoenergetic. However, ligation of the more electronegative nitrido ligand is thermodynamically favored over the alkyldiyne ligand when the metal is more electropositive.<sup>23</sup> This effect is observed in tungsten NACM catalysts **1** and **2**, where catalyst **1** prefers a nitride resting state while catalyst **2** prefers an alkyldiyne resting state.<sup>10</sup> As a more electronegative metal than tungsten in high oxidation states, molybdenum prefers alkyldiyne ligation more so than tungsten. This presents a second obstacle for molybdenum-catalyzed NACM since the nitride complex must be thermodynamically accessible from the alkyldiyne complex. In principle, the use of a stronger electron-donor ligand set than  $-\text{OCMe}(\text{CF}_3)_2$  should make the alkyldiyne-to-nitride conversion more thermodynamically favorable by stabilizing the nitride complex with respect to the alkyldiyne complex. However, this approach is problematic as it runs afoul of the increased kinetic barrier noted above;  $\text{N}\equiv\text{Mo}(\text{OCMe}_3)_3$  (**6**) and  $\text{N}\equiv\text{Mo}(\text{OCMe}_2\text{CF}_3)_3$  (**7**) do not react with alkynes to form alkyldiyne complexes.<sup>13,14</sup> Therefore, increasing the ancillary ligand electron-donor strength is not by itself likely to yield active molybdenum NACM catalysts.

Table 1. Alcohol pK<sub>a</sub> Values

alcohol	pK <sub>a</sub> (H <sub>2</sub> O)	pK <sub>a</sub> (DMSO)
Me <sub>3</sub> COH	19.2 <sup>a</sup>	32.2 <sup>b</sup>
(CF <sub>3</sub> )Me <sub>2</sub> COH	13.3 <sup>c</sup>	
(CF <sub>3</sub> ) <sub>2</sub> MeCOH	9.6 <sup>a</sup>	
(CF <sub>3</sub> ) <sub>3</sub> COH	5.4 <sup>a</sup>	10.7 <sup>d</sup>
PhOH	9.9 <sup>e</sup>	18.0 <sup>e</sup>
Ph <sub>3</sub> SiOH		16.6 <sup>f</sup>

<sup>a</sup> Ref 25. <sup>b</sup> Ref 26. <sup>c</sup> Ref 27. <sup>d</sup> Ref 28. <sup>e</sup> Ref 29. <sup>f</sup> Ref 30.

Scheme 3. Synthesis of Mo Aryloxy Complexes

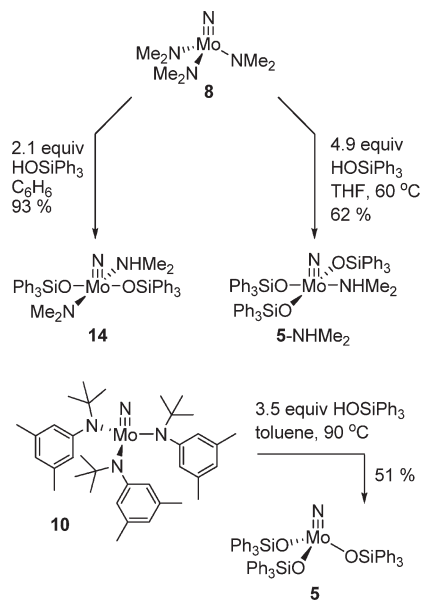


Given the apparent ability of alkoxide ligands to undergo C–O bond scission at elevated temperatures,<sup>24,10</sup> it was anticipated that more thermally robust ancillary ligands might be required to maintain catalyst integrity at the elevated temperatures necessary to overcome the larger intrinsic alkyldiene-to-nitride barrier with Mo-based catalysts. In order to retain the previously observed nitride-to-alkyldiene reactivity, the new ligands should have an electron-donor strength similar to that of  $-\text{OCMe}(\text{CF}_3)_2$ . Using the pK<sub>a</sub> of the parent alcohols (Table 1)<sup>25–30</sup> as an estimate for the electron donating ability of the corresponding alkoxide ligands, we chose to employ phenoxide, triphenylsiloxy, and alkyldiphenylsiloxy ligands in a search for potential NACM catalysts. The C(sp<sup>2</sup>)–O and Si–O bonds of these ligands should be stronger than the C(sp<sup>3</sup>)–O bonds of the fluorinated *tert*-butoxide ligands, thereby improving the stability of the molybdenum complexes. Because neutral donor ligands can inhibit the metathesis reaction, base-free complexes of the type  $\text{N}\equiv\text{Mo}(\text{OR})_3$  were targeted. Herein, we report our efforts in the synthesis of new Mo–nitride complexes and their activity in both ACM and NACM.

## RESULTS AND DISCUSSION

**Syntheses of Molybdenum–Nitride Complexes.** Protonolysis of  $\text{N}\equiv\text{Mo}(\text{NRR}')_3$  complexes with substituted phenols or silanols was found to be the best method of accessing the desired complexes. Bulky alcohols were employed in order to prevent oligomerization of the nitride complexes<sup>31</sup> and to minimize alkyne polymerization in the presence of alkyne substrates.<sup>20</sup> Three known complexes were employed as precursors:  $\text{N}\equiv\text{Mo}(\text{NMe}_2)_3$  (**8**),<sup>32</sup>  $\text{N}\equiv\text{Mo}[\text{N}(\text{Pr})\text{Ar}]_3$  (**9**),<sup>33</sup> and  $\text{N}\equiv\text{Mo}[\text{N}(\text{tBu})\text{Ar}]_3$  (**10**)<sup>34</sup>

Scheme 4. Synthesis of Mo Triphenylsiloxy Complexes

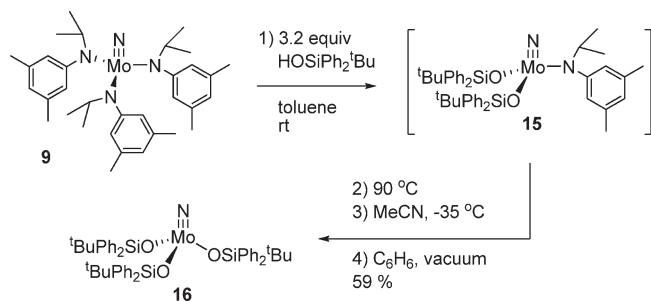


(Ar = 3,5-Me<sub>2</sub>C<sub>6</sub>H<sub>3</sub>). The reactivity of **8–10** with the different ligands varied, and so each ligand type will be considered in turn.

The synthesis of tris-aryloxy complexes using bulky phenols was investigated first. The addition of 1.1 equiv of 2,6-di-*tert*-butylphenol (HODTBP) to **8** resulted in the ready formation of  $\text{N}\equiv\text{Mo}(\text{ODTBP})(\text{NMe}_2)_2$  (**11**), which was isolated as a pale yellow powder in 81% yield by washing the crude product with cold pentane (Scheme 3). Further replacement of  $-\text{NMe}_2$  was not achieved by adding more equivalents of HODTBP to **8**, most likely due to the size of the  $-\text{ODTBP}$  ligand. The <sup>1</sup>H NMR spectrum of **11** displays two broadened  $-\text{NMe}_2$  resonances which sharpen at  $-10^\circ\text{C}$ , indicating hindered rotation about the Mo–NMe<sub>2</sub> bonds.

Treating **8** with an excess of the less hindered 2,6-di-*iso*-propylphenol (HODIPP) in THF at 60 °C results in the complete formation of  $\text{N}\equiv\text{Mo}(\text{ODIPP})_3(\text{NHMe}_2)$  (**12**) as judged by <sup>1</sup>H NMR spectroscopic analysis of the reaction mixture (Scheme 3). Isolation of pure **12** proved challenging due to its high solubility in both polar and nonpolar solvents. Ultimately, deep red crystals of **12** were grown from concentrated acetonitrile solutions at  $-35^\circ\text{C}$ . <sup>1</sup>H NMR spectroscopic analysis of the isolated bulk sample revealed the presence of  $\text{N}\equiv\text{Mo}(\text{ODIPP})_2(\text{NMe}_2)(\text{NHMe}_2)$  (**13**) as a minor component (9%) of **12**. The mechanism of reversion from **12** to **13** is unclear at present. The isolated mixture of **12** and **13** also contained 0.4 equiv of HODIPP as determined by <sup>1</sup>H NMR spectroscopy. Complex **12** displays a single  $-\text{OAr}$  environment in its <sup>1</sup>H NMR spectrum, indicating rapid exchange of the aryloxy ligands. Tris-anilide precursors **9** and **10** were found to react sluggishly with HODIPP at 60–90 °C, and no discernible products could be observed from this synthetic route. Steric congestion near the hydroxyl group of HODIPP likely prevents approach to the bulky anilide ligands of **9** and **10**.

The addition of 2.1 equiv of HOSiPh<sub>3</sub> to a benzene solution of **8** led to the precipitation of  $\text{N}\equiv\text{Mo}(\text{OSiPh}_3)_2(\text{NMe}_2)(\text{NHMe}_2)$  (**14**), which was isolated in 93% yield as a pale yellow powder (Scheme 4). Both the  $-\text{NMe}_2$  and  $-\text{NHMe}_2$  ligands displayed hindered rotation about the Mo–N bond on the <sup>1</sup>H NMR time

Scheme 5. Synthesis of Mo *tert*-Butyldiphenylsiloxide Complexes

scale. A *trans* square pyramidal geometry was assigned to **14** due to the absence of crosspeaks between the  $-\text{NMe}_2$  and  $-\text{NHMe}_2$  ligands in the 2D NOESY spectrum. Full siloxide substitution was achieved by treating **8** with 4.9 equiv of  $\text{HOSiPh}_3$  in THF at  $60^\circ\text{C}$ , resulting in the formation of  $\text{N}\equiv\text{Mo}(\text{OSiPh}_3)_3(\text{NHMe}_2)$  (**5-NHMe<sub>2</sub>**). Complex **5-NHMe<sub>2</sub>** was isolated as a white powder in 62% yield by precipitation from a concentrated THF/toluene solution. A single set of broadened  $-\text{OSiPh}_3$  resonances appeared in the  $^1\text{H}$  NMR spectrum of **5-NHMe<sub>2</sub>**, suggesting that ligand exchange in **5-NHMe<sub>2</sub>** is somewhat slower than in **12**. The base-free complex  $\text{N}\equiv\text{Mo}(\text{OSiPh}_3)_3$  (**5**) was formed by treating a toluene solution of **10** with 3.5 equiv of  $\text{HOSiPh}_3$  at  $90^\circ\text{C}$ .  $^1\text{H}$  NMR spectroscopic analysis indicated that the reaction proceeded cleanly to form **5** with no intermediates being observed. The addition of an excess of pentane to the reaction mixture caused the precipitation of **5** as a white powder in 51% yield.

The bulkier silanol  $\text{HOSiPh}_2^t\text{Bu}$  was found to react most rapidly with precursor **9** (Scheme 5). Treatment of a toluene solution of **9** with 3.2 equiv of  $\text{HOSiPh}_2^t\text{Bu}$  at room temperature led to the complete formation of  $\text{N}\equiv\text{Mo}(\text{OSiPh}_2^t\text{Bu})_2$  ( $\text{N}[\text{Pr}]\text{Ar}$ ) ( $\text{Ar} = 3,5\text{-Me}_2\text{C}_6\text{H}_3$ ) (**15**) as judged by  $^1\text{H}$  NMR spectroscopy. Heating this reaction mixture of unisolated **15** and excess silanol at  $90^\circ\text{C}$  resulted in a 79% conversion to  $\text{N}\equiv\text{Mo}(\text{OSiPh}_2^t\text{Bu})_3$  (**16**) after 3 h, with 21% of **15** remaining in solution. Further heating of the reaction mixture resulted in negligible change in the product composition. Cooling an acetonitrile solution of the crude mixture to  $-35^\circ\text{C}$  resulted in the precipitation of a gummy white solid, which was presumed to be an acetonitrile adduct of **16**. By reprecipitating the solid several times, dissolving it in benzene, then lyophilizing the benzene solution, pure **16** could be isolated as a yellow oil in 59% yield.

Attempts at crystallization of the solid tris-siloxide complexes (**5-NHMe<sub>2</sub>**, **5**) were unsuccessful, and so direct structural comparisons of these complexes cannot be made. It was found that 3.2 equiv of  $\text{HOCPh}_2\text{Me}$ , which is structurally similar to  $\text{HOSiPh}_2^t\text{Bu}$ , reacted with **8** in THF at room temperature to give  $\text{N}\equiv\text{Mo}(\text{OCPh}_2\text{Me})_3(\text{NHMe}_2)$  (**17-NHMe<sub>2</sub>**) as an initial product which crystallized readily from a toluene/pentane solution at  $-35^\circ\text{C}$  (Scheme 6). Complex **17-NHMe<sub>2</sub>** was not isolated in bulk but instead was precipitated again from toluene/pentane, resulting in the spontaneous loss of the  $\text{NHMe}_2$  ligand to give  $\text{N}\equiv\text{Mo}(\text{OCPh}_2\text{Me})_3$  (**17**) in 21% isolated yield.

**Structural Studies.** X-ray quality crystals of **12** were grown from an acetonitrile solution at  $-35^\circ\text{C}$ . Single-crystal X-ray diffraction analysis revealed that **12** crystallizes in the monoclinic space group  $P2_1/n$  (Figure 1). The  $\text{Mo}-\text{N}$  triple bond length is

## Scheme 6. Synthesis of Mo Diphenylethoxide Complexes

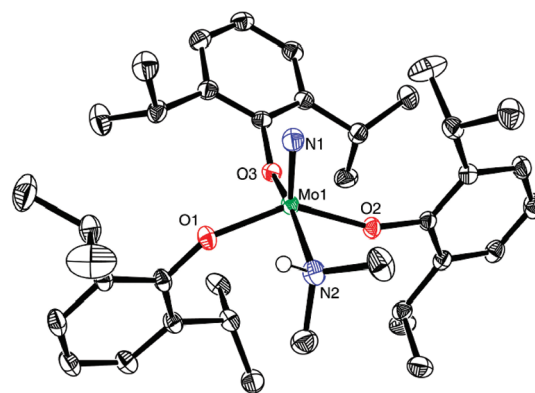
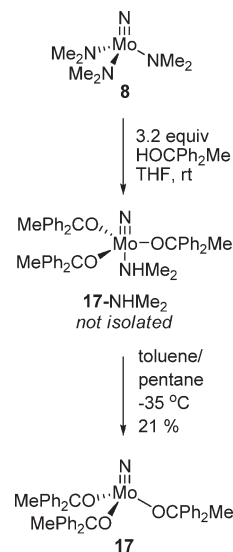


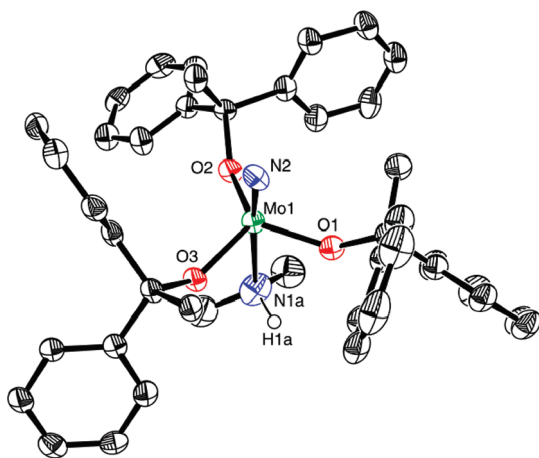
Figure 1. 50% thermal ellipsoid plot of **12**.

typical at  $1.6509(10)$  Å, and the  $\text{Mo}-\text{NHMe}_2$  bond length is  $2.2859(11)$  Å (Table 2). The mutually *trans* aryloxy rings lie approximately in a plane containing the  $\text{Mo}\equiv\text{N}$  bond, while the third aryloxy is approximately orthogonal to the plane. Calculation of the  $\tau$  parameter<sup>35</sup> for **12** results in a value of  $\tau = 0.37$ , indicating that **12** is best described as having a distorted square pyramidal geometry. Similar  $\tau$  values are calculated for the related complexes **4** ( $\tau = 0.22$ )<sup>14</sup> and **5-py** ( $\tau = 0.37$ ).<sup>12</sup>

X-ray quality crystals of **17-NHMe<sub>2</sub>** were grown from a toluene/pentane solution at  $-35^\circ\text{C}$ . Single-crystal X-ray diffraction analysis revealed that **17-NHMe<sub>2</sub>** crystallizes in the triclinic space group  $P\bar{1}$  (Figure 2). The dimethylamine ligand is rotationally disordered over two equally occupied positions and was confirmed to be located *trans* to the nitride ligand. The  $\text{Mo}-\text{N}$  bond for  $\text{NHMe}_2$  is very long at  $2.606(6)$  Å and  $2.584(6)$  Å for the two sites due to the *trans* influence of the nitride ligand (Table 2). Additionally, the  $\text{Mo}-\text{N}$  triple bond is quite long at  $1.700(4)$  Å, likely as a result of the *trans*  $\sigma$ -donor  $\text{NHMe}_2$  ligand. This distance is among the longest found for a terminal nitride complex of molybdenum.<sup>36</sup> Geometrical analysis of the structure yields  $\tau = 0.97$ , which is very close to an ideal trigonal bipyramid.<sup>35</sup>

Table 2. Selected Bond Lengths and Angles for **12** and **17-NHMe<sub>2</sub>**

12		17-NHMe <sub>2</sub>	
bond distances (Å)			
Mo–N(1)	1.6509(10)	Mo–N(2)	1.700(4)
Mo–N(2)	2.2859(11)	Mo–N(1a)	2.606(6)
Mo–O(1)	1.9292(8)	Mo–O(1)	1.883(3)
Mo–O(2)	1.9206(8)	Mo–O(2)	1.884(3)
Mo–O(3)	1.9333(8)	Mo–O(3)	1.883(3)
Bond Angles (deg)			
N(1)–Mo–O(1)	103.93(4)	N(2)–Mo–O(1)	102.18(15)
N(1)–Mo–O(2)	109.65(4)	N(2)–Mo–O(2)	104.19(15)
N(1)–Mo–O(3)	102.35(5)	N(2)–Mo–O(3)	103.01(15)
N(1)–Mo–N(2)	92.79(5)	N(2)–Mo–N(1a)	175.5(2)
O(1)–Mo–N(2)	81.34(4)	O(1)–Mo–O(2)	113.64(12)
O(1)–Mo–O(3)	95.12(4)	O(1)–Mo–O(3)	117.53(12)
O(2)–Mo–N(2)	81.49(4)	O(2)–Mo–O(3)	113.91(12)
O(2)–Mo–O(3)	92.97(3)	O(1)–Mo–N(1a)	74.0(2)
		O(2)–Mo–N(1a)	79.8(2)
		O(3)–Mo–N(1a)	77.07(18)

Figure 2. 50% thermal ellipsoid plot of **17-NHMe<sub>2</sub>**.

It is unusual to find the NHMe<sub>2</sub> ligand of **17-NHMe<sub>2</sub>** *trans* to the strong *trans*-influence nitride ligand. However, the solid state structure of **17-NHMe<sub>2</sub>** is consistent with the observed lability of the NHMe<sub>2</sub> ligand in **17-NHMe<sub>2</sub>**. Solutions of **12** do not lose coordinated NHMe<sub>2</sub>, which is found *cis* to the nitride ligand in the solid state. Because **5-NHMe<sub>2</sub>** also retains its NHMe<sub>2</sub> ligand in solution, it can be inferred by analogy to possess a *pseudo* square pyramidal structure similar to **12**.

**Alkyne Cross Metathesis.** Molybdenum nitride complexes have previously been observed to undergo the nitride-to-alkylidyne conversion,<sup>11</sup> which is half of the cycle required for NACM. Therefore, the ACM activity of the new complexes was investigated in order to assess their ability to form alkylidyne complexes. The unsymmetrical alkyne 1-phenyl-1-butyne was chosen as the test substrate. As seen in Figure 3, the ACM products of 1-phenyl-1-butyne are diphenylacetylene and 3-hexyne. The reaction progress was readily monitored by <sup>1</sup>H NMR spectroscopy through integration of the Ph group resonances. At a

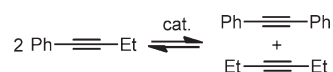


Figure 3. ACM test reaction.

statistical equilibrium mixture as shown in Figure 3, the integrations for 1-phenyl-1-butyne and diphenylacetylene would be equivalent.

The five new trialkoxide complexes N≡Mo(OR)<sub>3</sub>L (L = NHMe<sub>2</sub>: **12**, **5-NHMe<sub>2</sub>**; L = vacant site: **5**, **16**, **17**) were treated with 20 equiv of 1-phenyl-1-butyne in C<sub>6</sub>D<sub>6</sub>. Complexes **12** and **5-NHMe<sub>2</sub>** were both found to reach a statistical equilibrium of ACM products within 1.5–2.5 h at 75 °C, despite the presence of the basic NHMe<sub>2</sub> ligand (Table 3). Complex **5**, the base-free analogue of **5-NHMe<sub>2</sub>**, is much more active for ACM with products appearing after only minutes at room temperature. Reactions catalyzed by **5** reach a statistical equilibrium of products after only 1.5 h at room temperature. No benzonitrile or propionitrile could be observed in the <sup>1</sup>H NMR spectra of ACM mixtures catalyzed by **5** at room temperature, which suggests only trace formation of a catalytically active alkylidyne species. This behavior is not specific to **5**, as similar activity has been observed for **3** and **4**.<sup>14</sup> When ACM mixtures of **5** were heated to 90 °C for 16 h, an 80% conversion to one or more new complexes was observed in the <sup>1</sup>H NMR spectrum along with a stoichiometric amount of propionitrile. Although the formation of propionitrile suggests that this new species be assigned as PhC≡Mo(OSiPh<sub>3</sub>)<sub>3</sub> or EtC≡Mo(OSiPh<sub>3</sub>)<sub>3</sub>, no signals characteristic of either an alkylidyne or benzylidyne complex were observed by <sup>13</sup>C NMR spectroscopy. One explanation for this is a thermal instability of RC≡Mo(OSiPh<sub>3</sub>)<sub>3</sub>, as reported for the diethyl ether adduct.<sup>15</sup> At present, the identity of the molybdenum-containing product remains unknown.

The observed ACM activity for isolated **5** is in apparent contrast to previous studies of **5** that was generated in situ from the reaction of N≡Mo(N(SiMe<sub>3</sub>)<sub>2</sub>)(OSiMe<sub>3</sub>)<sub>2</sub> with Ph<sub>3</sub>SiOH.<sup>15</sup> In these studies, **5** was reported to be unreactive with 5-decyne at room temperature on the basis of the absence of valeronitrile in the <sup>1</sup>H NMR spectrum.<sup>15</sup> However, under these conditions, trace formation of an alkylidyne species would not have been detected, as only degenerate ACM would occur; thus, no new alkynes would be formed and ACM would not be observed by <sup>1</sup>H NMR spectroscopy. Additionally, in situ generated **5** was reported to afford only small amounts of the metathesis product valeronitrile after 6 days at 100 °C.<sup>15</sup> In the present case, the reaction of isolated **5** with 1-phenyl-1-butyne may be facilitated by the formation of a benzylidyne complex, which in general is thermodynamically preferred over alkylidyne complexes.<sup>10,20,37</sup> In any event, the reaction of pure **5** with 1-phenyl-1-butyne proceeds to a much greater extent in a shorter time at lower temperatures with less polymerization than did **5** prepared in situ with 5-decyne.

While **5** was highly active for ACM, **16** was completely inactive for ACM up to 90 °C. Steric interactions of the larger –OSi<sup>t</sup>BuPh<sub>2</sub> ligand are likely to increase the activation barrier for metalacycle formation in **16** relative to **5**. However, the degree that steric effects contribute to the inactivity of **16** is unknown. Inductive effects of the <sup>t</sup>Bu group should render –OSi<sup>t</sup>BuPh<sub>2</sub> a stronger electron donor ligand than –OSiPh<sub>3</sub>, and so electronic effects could also contribute to the reactivity differences between **5** and **16**. A pK<sub>a</sub> value for HOSi<sup>t</sup>BuPh<sub>2</sub> would be useful for a comparison of relative electron–donor

Table 3. ACM of 1-Phenyl-1-butyne with  $N\equiv Mo(OR)_3L^a$ 

complex	OR	L	temp/ $^{\circ}C$	time/h <sup>b</sup>	% PhCCEt	% PhCCPh	% EtCCEt
12	ODIPP	NHMe <sub>2</sub>	75	2.5	50	25	25
5-NHMe <sub>2</sub>	OSiPh <sub>3</sub>	NHMe <sub>2</sub>	75	1.5	50	25	25
5	OSiPh <sub>3</sub>		RT <sup>c</sup>	1.5	50	25	25
16	OSi <sup>t</sup> BuPh <sub>2</sub>		90	9.0 <sup>d</sup>	100	0	0
17	OCMePh <sub>2</sub>		75	21.0 <sup>d</sup>	100	0	0

<sup>a</sup> NMR scale reactions with 5 mol % catalyst at a catalyst concentration of 10 mg mL<sup>-1</sup> in C<sub>6</sub>D<sub>6</sub>. Product compositions were determined from integration of the <sup>1</sup>H NMR spectrum resonances relative to an internal 1,3,5-trimethoxybenzene reference. <sup>b</sup> Time to reaction completion in hours. <sup>c</sup> RT = room temperature. <sup>d</sup> No reaction was observed during this time period.

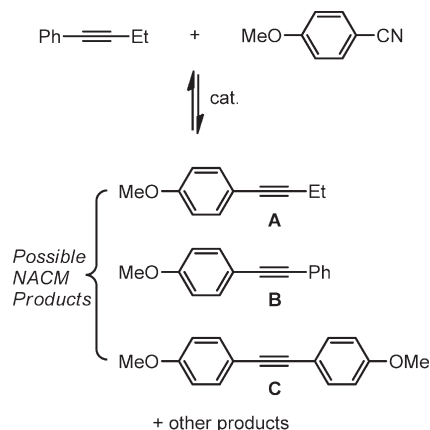


Figure 4. NACM test reaction.

abilities but has not been reported in the literature. However, the similar  $pK_a$ 's of HOSiPh<sub>3</sub> ( $pK_a = 16.57$ , DMSO)<sup>30</sup> and HOCPh<sub>3</sub> ( $pK_a = 16.97$ , DMSO)<sup>30</sup> suggest that  $-OSi^tBuPh_2$  and its carbon analogues possess similar electron donor strengths. Accordingly, 17 is also inactive for ACM at 75  $^{\circ}C$ , while rapid decomposition to 1,1-diphenylethene is observed at higher temperatures. This lack of ACM activity for 17 suggests that electronic factors play at least a partial role in the inactivity of 16 toward ACM.

**Nitrile-Alkyne Cross Metathesis.** With an understanding of their ACM activity in hand, the complexes were next tested for NACM. The complexes were heated with 10 equiv of 1-phenyl-1-butyne to initiate alkyldiyne formation and 10 equiv of anisonitrile to complete the NACM cycle. Incorporation of a *p*-methoxyphenyl unit into any one of the three alkyne products A–C (Figure 4) would be evidence for successful NACM, as each of these products necessitates metathesis between an alkyldiyne complex and a nitrile. Anisonitrile was chosen as the nitrile substrate for two reasons. First, resonances for both the OCH<sub>3</sub> and ArH (*ortho* to MeO) are not obscured by other peaks in the <sup>1</sup>H NMR spectrum of the proposed reaction mixture. Second, in NACM reactions catalyzed by 1, anisonitrile is significantly more reactive for NACM than most other nitrile substrates tested.<sup>9,10</sup> Therefore, if a complex does not catalyze NACM of anisonitrile, then it is not expected to catalyze NACM for most substrates.

During the course of the NACM survey,  $N\equiv Mo(OSiPh_3)_3$  (5) was discovered to be active for NACM at a temperature of 180–185  $^{\circ}C$  in solutions of BrC<sub>6</sub>D<sub>5</sub>. Both 1-(but-1-ynyl)-4-methoxybenzene (A) and 1-methoxy-4-(phenylethynyl)benzene (B) were observed in the <sup>1</sup>H NMR spectrum, and their identities were further confirmed by GC-MS. As seen in Figure 5,

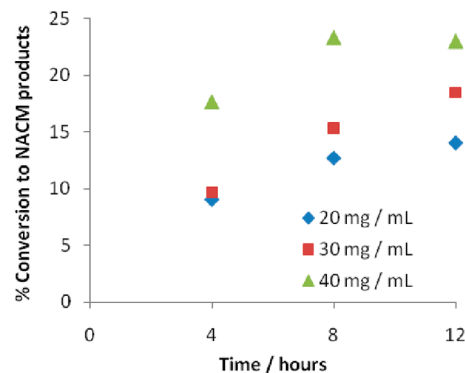


Figure 5. Conversion to NACM products at different concentrations of 5.

increasing the concentration of 5 from 20 mg mL<sup>-1</sup> (21 mM) to 40 mg mL<sup>-1</sup> (43 mM) resulted in both faster and higher conversion to NACM products. Greater than 20% conversion to NACM products is obtained over 8 h, which corresponds to slightly more than two turnovers with respect to 5. However, the catalyst was deactivated during the course of the reaction; thus, a true equilibrium is never established. Decomposition of the alkyldiyne form of the catalyst likely accounts for the loss of catalyst as 5 decomposes only slightly upon heating at 180  $^{\circ}C$  for 16 h in a BrC<sub>6</sub>D<sub>5</sub> solution. The NACM substrate scope of 5 was not pursued due to the poor reactivity of anisonitrile in this system.

That nitriles undergo rapid ligand exchange at the molybdenum center was established by adding 1–10 equivalents of MeCN to 5 in C<sub>6</sub>D<sub>6</sub>. Even at room temperature, only one signal for the CH<sub>3</sub> group was observed in every case. This signal shifted smoothly downfield toward the value for free MeCN as the number of equivalents was increased. Interestingly, in spite of the ACM and NACM activity demonstrated by 5, no degenerate N-atom exchange<sup>21,22</sup> was observed when labeled <sup>15</sup>N-CMe was added to a mixture of 5 and anisonitrile, even after 60 h at 80  $^{\circ}C$  in C<sub>6</sub>D<sub>6</sub>.

It was observed that the NACM activity of 5 ceases prior to complete catalyst decomposition, as both the nitride and a new species were observed in the <sup>1</sup>H NMR spectrum of the NACM-inactive reaction mixtures. At low catalyst concentrations (20–30 mg mL<sup>-1</sup>), productive NACM was observed over 12 h, while at a higher concentration (40 mg mL<sup>-1</sup>), NACM was observed only over 8 h. The NACM inhibition may arise from the presence of decomposition products in the reaction mixture. However, the decomposition products are unknown, and therefore possible modes of catalyst inhibition are presently unclear.

Table 4. ACM and NACM Activity of Mo Complexes<sup>a</sup>

complex	R	L	time (h)	ACM	NACM	cat. decomp.
12	ODIPP	NHMe <sub>2</sub>	4	Y	N	100%
5-NHMe <sub>2</sub>	OSiPh <sub>3</sub>	NHMe <sub>2</sub>	20	Y	N	100%
5-py <sup>b</sup>	OSiPh <sub>3</sub>	py	12	Y	Y <sup>c</sup>	... <sup>d</sup>
5	OSiPh <sub>3</sub>		12	Y	Y	66%
16	OSi <sup>t</sup> BuPh <sub>2</sub>		8	Y <sup>e,f</sup>	N	17%
6	OCMe <sub>3</sub>		4	Y <sup>e,g</sup>	N	100%
7	OCMe <sub>2</sub> CF <sub>3</sub>		16	Y <sup>e,h</sup>	N	49%
3	OCMe(CF <sub>3</sub> ) <sub>2</sub>		4	Y	N	100%
4	OC(CF <sub>3</sub> ) <sub>3</sub>	NcMe	4	Y	N	100%

<sup>a</sup>NMR scale reactions with 10 equiv of 1-phenyl-1-butyne and 10 equiv of anisonitrile at a catalyst concentration of 40 mg mL<sup>-1</sup> in BrC<sub>6</sub>D<sub>5</sub> at 180 °C. <sup>b</sup>Generated *in situ* by treatment of 5 with 1 equiv of pyridine. <sup>c</sup>A 14% conversion to NACM products was observed. <sup>d</sup>Not determined. <sup>e</sup>Does not catalyze ACM at ≤90 °C. <sup>f</sup>Alkyne distribution: 54% 1-phenyl-1-butyne, 23% diphenylacetylene, 23% 3-hexyne. <sup>g</sup>Statistical equilibrium of alkyne products. <sup>h</sup>Alkyne distribution: 44% 1-phenyl-1-butyne, 28% diphenylacetylene, 28% 3-hexyne.

Other molybdenum nitride complexes were tested for NACM using the optimized conditions of 5 (40 mg mL<sup>-1</sup>; Table 4). Complexes 12 and 5-NHMe<sub>2</sub>, which were sluggish ACM catalysts due to the presence of the NHMe<sub>2</sub> ligand, displayed ACM activity as expected but no NACM activity. Complex 12 was clearly unstable to the reaction conditions, as free HODIPP was the only observable phenolic species after 4 h of reaction. The time taken for decomposition of 5-NHMe<sub>2</sub> was difficult to ascertain directly from the <sup>1</sup>H NMR spectrum. After 20 h of reaction, no NACM products were observed. The addition of extra 1-phenyl-1-butyne to the reaction mixture did not result in further ACM, indicating that 5-NHMe<sub>2</sub> had been completely deactivated. The known complex N≡Mo(OSiPh<sub>3</sub>)<sub>3</sub>(py) (5-py) was found to be active for NACM under the optimized conditions, with a 14% conversion to NACM products observed after 12 h. Notably, 5-py generates greater amounts of insoluble poly(3-hexyne) as a byproduct than does 5. After 12 h under the optimized NACM conditions, solutions of 5-py lost 72% of the total Et group signal intensity, while solutions of 5 lost only 47%. NACM solutions of 5-py become quite viscous due to the amount of polymer generated, which likely decreases molecular diffusion rates and inhibits NACM. Thus replacement of an NHMe<sub>2</sub> ligand with a more labile pyridine ligand allows NACM to occur, but at lower efficiency than the base-free complex 5.

Complex 16 did not produce any observable NACM products, though ACM products were observed in near statistical equilibrium under these reaction conditions. A trace amount of EtCN was observed in the <sup>1</sup>H NMR spectrum, which suggests trace formation of an unobserved alkyldiyne species that is highly active for ACM. The lack of NACM reactivity by the alkyldiyne complex could be due to a high energy barrier for azametallacycle formation, fast alkyldiyne complex decomposition, or insufficient concentration of the alkyldiyne complex. The nitride complex 16 is very stable under these conditions, with only 17% decomposition of 16 being observed over 8 h.

Nitride complexes containing *tert*-butoxide derived ligands were also inactive for NACM under these conditions. The highly fluorinated complexes 3 and 4 decomposed rapidly under the reaction conditions as determined by <sup>19</sup>F NMR spectroscopy, though ACM products were observed in accord with previously

known reactivity.<sup>11</sup> In contrast to previous observations, the less fluorinated complexes 6 and 7 also afforded ACM products in near statistical equilibria. A trace amount of EtCN was observed in the <sup>1</sup>H NMR spectrum of reactions catalyzed by 7, though no direct evidence of an alkyldiyne intermediate was observed for either complex. Complex 6 completely decomposes within 4 h under the reaction conditions, while 7 is remarkably stable with only 49% catalyst decomposition occurring over 16 h. Similar to 16, the increase in reaction temperature from 90 to 185 °C is sufficient to overcome the energy barrier for metallocycle formation from 6 and 7, though the rate of reaction is slow compared to that for tungsten catalysts 1 and 2.

The *tert*-butoxide derived complexes are unstable at these elevated temperatures as originally anticipated, though no olefinic byproducts were observed that would suggest that the mechanism of decomposition involved C–O bond scission. In the case of 7, the only observable ligand-derived decomposition product was HOOCMe<sub>2</sub>CF<sub>3</sub>. Free ligand-derived alcohol is observable for 3, 4, and 6, though a variety of other unidentified decomposition products were also produced.

## CONCLUSION

In summary, protonolysis of N≡Mo(NRR')<sub>3</sub> complexes serves as an efficient means to synthesize a variety of molybdenum nitride complexes containing bulky aryloxy and siloxy ligands. Differing reactivity of the various tris-amido precursors with each alcohol demonstrates the fine balance between the size of both the amido ligand and the incoming alcohol. Complexes 12 and 5-NHMe<sub>2</sub>, which contain weak electron-donor ligands, were found to retain NHMe<sub>2</sub> as a ligand, while the less Lewis-acidic 17-NHMe<sub>2</sub> was found to spontaneously evolve NHMe<sub>2</sub> to generate 17. The base-free complexes 5 and 16 were therefore made by the protonolysis of bulky amido groups.

Complexes 12, 5-NHMe<sub>2</sub>, and 5 were all shown to catalyze ACM efficiently within hours at 75 °C or less, with the base-free complex 5 being highly active even at room temperature. Complexes 16 and 17, which contain stronger electron-donor ligands, were inactive for ACM at temperatures typically employed for ACM with molybdenum nitride complexes. However, all molybdenum nitride complexes tested were precatalysts for ACM at 180 °C in bromobenzene, though varying degrees of catalyst decomposition were noted, and 7 and 16 failed to provide the equilibrium distribution of alkynes. NACM was achieved with 5 at elevated reaction temperatures of 180 °C, though conversion to NACM products was low before catalyst decomposition led to inhibition of the catalytic cycle. Inclusion of the weak base pyridine slowed the NACM reaction, while the stronger base NHMe<sub>2</sub> prevented NACM from occurring. Other molybdenum nitride complexes were found to be inactive for NACM under similar conditions.

From the above study, it is apparent that the NACM reaction is inherently more difficult to achieve with molybdenum complexes than with tungsten. However, less demanding ACM can be achieved with many molybdenum-nitrido complexes, though high temperatures may be needed in the absence of a Lewis acid cocatalyst to facilitate initial nitride-to-alkyldiyne exchange.<sup>38</sup> The –OSiPh<sub>3</sub> ligand provides an appropriate combination of electronics and thermal stability to allow NACM to occur, though significant catalyst improvement is needed to make a desirable molybdenum NACM catalyst. Improved molybdenum catalysts for NACM will be reported in due course.

## EXPERIMENTAL SECTION

**General Procedures.** All reactions were performed in a nitrogen-filled MBRAUN Labmaster 130 glovebox.  $^1\text{H}$  NMR spectra were recorded at 499.909 MHz, 399.967 MHz, or 300.075 MHz on a Varian Inova 500, Varian Inova 400, Varian MR400, or Varian Inova 300 spectrometer and referenced to the residual protons in  $\text{CDCl}_3$  (7.26 ppm), bromobenzene- $d_5$  (7.18 ppm),  $\text{C}_6\text{D}_6$  (7.16 ppm),  $\text{CD}_2\text{Cl}_2$  (5.32 ppm), or toluene- $d_8$  (2.09 ppm).  $^{13}\text{C}$  NMR spectra were recorded at 100.724 MHz on a Varian Inova 400 or Varian MR400 spectrometer and were referenced to naturally abundant  $^{13}\text{C}$  nuclei in  $\text{CDCl}_3$  (77.16 ppm),  $\text{C}_6\text{D}_6$  (128.06 ppm), toluene- $d_8$  (125.49), or  $\text{CD}_2\text{Cl}_2$  (54.00 ppm). GC/MS data were collected on a Shimadzu GCMS-QP5000 with a Restek XTI-5 phase column (30 m, 0.25 I.D., 0.25 D. F.). EI-MS data were collected on a VG (Micromass) 70–250-S magnetic sector mass spectrometer. Combustion analyses were performed by Midwest Microlabs, LLC.

**Materials and Methods.** All bulk solvents were obtained from VWR scientific. Benzene and  $\text{CH}_2\text{Cl}_2$  were degassed and dried over 4 Å molecular sieves, and all other solvents used were dried and deoxygenated using the method of Grubbs et al.<sup>39</sup> The reagents  $\text{HOSiPh}_3$ ,<sup>40</sup>  $\text{Zr}(\text{NMe}_2)_4$ ,<sup>41</sup>  $\text{NMo}(\text{OC}(\text{CF}_3)_2\text{Me})_3$  (**3**),<sup>21</sup>  $\text{NMo}(\text{OC}(\text{CF}_3)_3)_3(\text{NCMe})$  (**4**),<sup>21</sup>  $\text{NMo}(\text{O}^t\text{Bu})_3$  (**6**),<sup>31</sup>  $\text{NMo}(\text{OC}(\text{CF}_3)_2\text{Me})_3$  (**7**),<sup>13</sup>  $\text{NMo}[\text{N}^i\text{Pr}-(3,5\text{-Me}_2\text{C}_6\text{H}_3)]_3$  (**9**),<sup>33</sup> and  $\text{NMo}[\text{N}^i\text{Bu}-(3,5\text{-Me}_2\text{C}_6\text{H}_3)]_3$  (**10**)<sup>34</sup> were all made according to literature procedures. NMR solvents were obtained from Cambridge Isotope Laboratories and were dried over 4 Å molecular sieves for at least 24 h. Anisotrile and 2,6-di-*tert*-butylphenol were obtained from Acros. 1-Phenyl-1-butyne was obtained from GFS Chemicals. 1,3,5-Trimethoxybenzene was obtained from Aldrich. 2,6-Diisopropylphenol was obtained from Alfa Aesar. 1,1-Diphenylethanol was obtained from TCI. Triphenylsilanol was obtained from Gelest. 1-Phenyl-1-butyne and 2,6-diisopropylphenol were dried for 24 h using 4 Å molecular sieves. All other reagents were used as received.

**Complex Syntheses.**  $\text{NMo}(\text{NMe}_2)_3$  (**8**). In a modification of the literature procedure,<sup>32</sup> solid  $\text{Zr}(\text{NMe}_2)_4$  (1.8886 g, 7.06 mmol, 0.85 equiv) was added to a stirring solution of **6** (2.7373 g, 8.31 mmol, 1.0 equiv) in toluene (110 mL). After stirring for 2 h, the solution was concentrated *in vacuo* to a volume of ca. 25 mL. Pentane (40 mL) was added, and the resulting precipitate was collected by vacuum filtration, washed with pentane, and dried *in vacuo* to give **8** (1.1844 g, 4.89 mmol, 59%) as a yellow powder. The filtrate was concentrated to dryness; then the residue was slurried in pentane (20 mL). The mixture was filtered, and the solid was washed with pentane ( $3 \times 5$  mL) and dried *in vacuo* to give a second crop of **8** (0.3690 g, 1.52 mmol, 18%).  $^1\text{H}$  NMR matched the literature values.

$\text{NMo}(\text{O}-2,6\text{-}^i\text{Pr}_2\text{C}_6\text{H}_3)(\text{NMe}_2)_2$  (**11**). Solid 2,6-di-*tert*-butylphenol (0.2783 g, 1.349 mmol, 1.1 equiv) was added to a stirring solution of **8** (0.3017 g, 1.246 mmol, 1.0 equiv) in THF (12 mL). After stirring for 5 h 30 min, the volatiles were removed *in vacuo*; then the residue was slurried in cold pentane (4 mL) and cooled to  $-35$  °C. The mixture was filtered, and the solid was washed with cold pentane ( $3 \times 1$  mL) and dried *in vacuo* to give **11** (0.4065 g, 1.008 mmol, 81%) as a pale yellow powder.  $^1\text{H}$  NMR (400 MHz,  $\text{C}_7\text{D}_8$ ,  $-10$  °C):  $\delta$  7.36 (d, 2H, ArH,  $^3J_{\text{H-H}} = 7.8$  Hz), 6.96 (t, 1H, ArH,  $^3J_{\text{H-H}} = 7.8$  Hz), 3.86 (s, 6H,  $\text{NCH}_3$ ), 2.83 (s, 6H,  $\text{NCH}_3$ ), 1.52 (s, 18H,  $\text{C}(\text{CH}_3)_3$ ).  $^{13}\text{C}\{^1\text{H}\}$  NMR ( $\text{C}_7\text{D}_8$ ,  $-10$  °C):  $\delta$  165.11, 139.05, 137.82, 120.61, 60.67, 44.62, 35.52, 31.58. Anal. Calcd for  $\text{C}_{182}\text{H}_{33}\text{MoN}_3\text{O}$ : C, 53.59; H, 8.25; N, 10.42. Found: C, 53.21; H, 8.02; N, 10.22.

$\text{NMo}(\text{O}-2,6\text{-}^i\text{Pr}_2\text{C}_6\text{H}_3)(\text{NHMe}_2)$  (**12**). Complex **8** (0.4150 g, 1.71 mmol, 1.0 equiv) was dissolved in THF (20 mL) inside of a bomb flask. Neat 2,6-diisopropylphenol (2.16 mL, 8.58 mmol, 5.0 equiv) was added to the THF solution. The bomb flask was sealed and heated at 60 °C with stirring for 11 h 30 min.  $^1\text{H}$  NMR of an aliquot indicated complete conversion to **12**. The solution was concentrated to dryness; then the

residue was dissolved in MeCN (3 mL) and cooled to  $-35$  °C. After 14 days, no crystals had formed. A seed crystal of **12** was added and the solution cooled to  $-35$  °C. After 23 days, the mother liquor was removed *via* pipet, leaving behind deep red crystals. The crystals were dissolved in  $\text{C}_6\text{H}_6$  (5 mL) and the solution frozen and lyophilized *in vacuo* to give crude **12** (0.4712 g, 1.456 mmol, 85%) as a deep red powder.  $^1\text{H}$  NMR analysis indicated the presence of 0.1 equiv of  $\text{NMo}(\text{O}-2,6\text{-}^i\text{Pr}_2\text{C}_6\text{H}_3)_2(\text{NMe}_2)(\text{NHMe}_2)$  (**13**) and 0.4 equiv of 2,6-diisopropylphenol.  $^1\text{H}$  NMR (500 MHz,  $\text{C}_6\text{D}_6$ ):  $\delta$  7.14 (d, 6H, ArH (**12**),  $^3J_{\text{H-H}} = 7.5$  Hz), 7.02 (d, 0.9H, ArH (HOAr),  $^3J_{\text{H-H}} = 7.6$  Hz), 6.98 (t, 3H, ArH (**12**),  $^3J_{\text{H-H}} = 7.5$  Hz), 6.92 (t, 0.4H, ArH (HOAr),  $^3J_{\text{H-H}} = 7.6$  Hz), 4.31 (s, 0.4H, OH (HOAr)), 3.94 (s, 0.5H,  $\text{NCH}_3$  (**13**)), 3.87 (br s, 6H,  $\text{CHMe}_2$  (**12**)), 2.93 (sep, 0.7H,  $\text{CHMe}_2$  (**13**),  $^3J_{\text{H-H}} = 6.8$  Hz), 2.82 (s, 0.5H,  $\text{NCH}_3$  (**13**)), 2.39 (sep, 0.7H,  $\text{CHMe}_2$  (HOAr),  $^3J_{\text{H-H}} = 6.1$  Hz), 2.02 (s, 3H,  $\text{NHCH}_3$  (**12**)), 2.01 (s, 3H,  $\text{NHCH}_3$  (**12**)), 1.37 (d, 1.3H,  $\text{CHCH}_3$  (**13**),  $^3J_{\text{H-H}} = 6.9$  Hz), 1.35 (d, 1.3H,  $\text{CHCH}_3$  (**13**),  $^3J_{\text{H-H}} = 6.9$  Hz), 1.29 (d, 36H,  $\text{CHCH}_3$  (**12**),  $^3J_{\text{H-H}} = 6.8$  Hz), 1.14 (d, 4.6H,  $\text{CHCH}_3$  (HOAr),  $^3J_{\text{H-H}} = 6.8$  Hz).  $^{13}\text{C}\{^1\text{H}\}$  NMR ( $\text{C}_6\text{D}_6$ , **12**):  $\delta$  161.09, 138.75, 124.65, 123.81, 42.63, 27.75, 24.81. EI/MS  $[\text{M}/\text{Z}]^+$ : 643.8 ( $\text{NMo}(\text{O}-2,6\text{-}^i\text{Pr}_2\text{C}_6\text{H}_3)_3$ ).

$\text{NMo}(\text{OSiPh}_3)_2(\text{NMe}_2)(\text{NHMe}_2)$  (**14**). Solid  $\text{HOSiPh}_3$  (0.3728 g, 1.349 mmol, 2.1 equiv) was added to a stirring solution of **8** (0.1554 g, 0.642 mmol, 1.0 equiv) in  $\text{C}_6\text{H}_6$  (5 mL). The solution immediately changed to a bright yellow color, which faded as a precipitate formed. After stirring for 1 h 15 min, pentane (10 mL) was added to the mixture, and the precipitate was collected by filtration, washed with pentane (5 mL), and dried *in vacuo* to yield **14** (0.4778 g, 0.597 mmol, 93%) as a pale yellow powder.  $^1\text{H}$  NMR (500 MHz,  $\text{CD}_2\text{Cl}_2$ ):  $\delta$  7.71–7.69 (m, 11H), 7.42–7.34 (m, 16H), 3.68 (s, 3H,  $-\text{NCH}_3$ ), 2.88 (s, 3H,  $-\text{NCH}_3$ ), 2.33 (s, 3H,  $\text{NHCH}_3$ ), 2.32 (s, 3H,  $\text{NHCH}_3$ ), 2.27 (br s, 1H,  $\text{NHMe}_2$ ).  $^{13}\text{C}\{^1\text{H}\}$  NMR ( $\text{CD}_2\text{Cl}_2$ ):  $\delta$  138.94, 135.83, 129.92, 128.26, 62.40, 46.88, 40.90. Anal. Calcd for  $\text{C}_{40}\text{H}_{43}\text{MoN}_3\text{O}_2\text{Si}_2$ : C, 64.07; H, 5.78; N, 5.60. Found: C, 64.02; H, 5.75; N, 5.40.

$\text{NMo}(\text{OSiPh}_3)_3(\text{NHMe}_2)$  (**5-NHMe**). A solid mixture of **8** (0.1343 g, 0.555 mmol, 1.0 equiv) and  $\text{HOSiPh}_3$  (0.4756 g, 1.72 mmol, 3.1 equiv) was dissolved in THF (10 mL) inside a bomb flask. The flask was placed in a 60 °C oil bath, and the reaction solution was stirred for 20 h.  $^1\text{H}$  NMR analysis of an aliquot revealed the presence of a small amount of remaining **14**. Additional  $\text{HOSiPh}_3$  (0.2760 g, 1.00 mmol, 1.8 equiv) was added to the reaction solution, which was then stirred at 60 °C for an additional 18 h.  $^1\text{H}$  NMR analysis of a second aliquot revealed the consumption of **14**. The reaction solution was pipetted into toluene (60 mL) with vigorous stirring, but no precipitate formed. The solution was concentrated *in vacuo* to a volume of ca. 10 mL, resulting in the precipitation of a powder. The solid was collected by vacuum filtration, washed with toluene ( $3 \times 5$  mL) and pentane (10 mL), then dried *in vacuo* to yield **5-NHMe** (0.3363 g, 0.343 mmol, 62%) as a white powder.  $^1\text{H}$  NMR analysis revealed the presence of a small amount of  $\text{HOSiPh}_3$ . The first crop of **15** was dissolved in  $\text{CH}_2\text{Cl}_2$  (10 mL), then  $\text{Et}_2\text{O}$  (8 mL) was added and the solution cooled to  $-35$  °C, resulting in the precipitation of a white powder. The powder was collected by vacuum filtration, washed with toluene ( $2 \times 10$  mL) and pentane ( $2 \times 10$  mL), then dried *in vacuo* to afford **15** (0.2512 g, 0.256 mmol, 46%).  $^1\text{H}$  NMR analysis of the second crop revealed no improvement in purity over the first crop of **5-NHMe**.  $^1\text{H}$  NMR (500 MHz,  $\text{CD}_2\text{Cl}_2$ ):  $\delta$  7.58 (br s, 15H, ArH), 7.29 (br s, 8H, ArH), 7.13 (br s, 15H), 2.54 (br s, 1H,  $\text{NHMe}_2$ ), 1.91 (s, 6H,  $\text{NH}(\text{CH}_3)_2$ ).  $^{13}\text{C}\{^1\text{H}\}$  NMR ( $\text{CD}_2\text{Cl}_2$ ):  $\delta$  136.85, 136.06, 130.14, 128.23, 41.77. EI/MS  $[\text{M}/\text{Z}]^+$ : 936.9 ( $\text{NMo}(\text{OSiPh}_3)_3$ ).

$\text{NMo}(\text{OSiPh}_3)_3$  (**5**). Complex **10** (0.2889 g, 0.452 mmol, 1.0 equiv) and  $\text{HOSiPh}_3$  (0.4392 g, 1.589 mmol, 3.5 equiv) were dissolved in toluene (20 mL) inside a bomb flask. The flask was heated in a 90 °C oil bath for 5 h 30 min, then cooled. Pentane (25 mL) was added to the solution with vigorous stirring; then the solution was allowed to settle.

No precipitate formed over 10 min, so additional pentane (5 mL) was added. The solution became cloudy and was allowed to settle overnight at  $-35\text{ }^{\circ}\text{C}$ . The powder was then collected by vacuum filtration, washed with  $\text{Et}_2\text{O}$  ( $3 \times 15\text{ mL}$ ), and dried *in vacuo* to afford **5** (0.2146 g, 0.229 mmol, 51%) as a white powder.  $^1\text{H NMR}$  (400 MHz,  $\text{C}_6\text{D}_6$ ):  $\delta$  7.67 (d, 18H, ArH,  $^3J_{\text{H-H}} = 7.1\text{ Hz}$ ), 7.16 (m, ArH), 7.06 (t, 17H, ArH,  $^3J_{\text{H-H}} = 7.5\text{ Hz}$ ).  $^{13}\text{C}\{^1\text{H}\}$  NMR ( $\text{C}_6\text{D}_6$ ):  $\delta$  135.87, 134.80, 130.45, 128.29. Anal. Calcd for  $\text{C}_{54}\text{H}_{45}\text{MoNO}_3\text{Si}_3$ : C, 69.28; H, 4.85; N, 1.50. Found: C, 69.04; H, 4.84; N, 1.47.

$\text{NMo}(\text{OSiPh}_2\text{Bu})_3$  (**16**). Complex **9** (0.2777 g, 0.465 mmol, 1.0 equiv) and  $\text{HOSiPh}_2\text{Bu}$  (0.3837 g, 1.496 mmol, 3.2 equiv) were dissolved in toluene (15 mL) inside a bomb flask. The flask was heated in a  $90\text{ }^{\circ}\text{C}$  oil bath for 10 h; then the flask was cooled and the volatiles removed *in vacuo*. The resulting oil was dissolved in MeCN (3 mL) and cooled to  $-35\text{ }^{\circ}\text{C}$ . A semisolid mass precipitated over several days; then the mother liquor was removed via pipet and the solid rinsed with cold MeCN (2 mL). The solid was redissolved in MeCN, and the precipitation procedure was repeated twice more. The resulting solid was dissolved in  $\text{C}_6\text{H}_6$  (6 mL); then the solution was frozen, lyophilized, and dried *in vacuo* to yield **16** (242.2 mg, 0.276 mmol, 59%) as a dark yellow oil.  $^1\text{H NMR}$  (500 MHz,  $\text{C}_6\text{D}_6$ ):  $\delta$  7.84–7.82 (m, 12H, ArH), 7.18–7.14 (m, ArH), 7.13–7.09 (m, 12H, ArH), 1.19 (s, 27H, C-( $\text{CH}_3$ )<sub>3</sub>).  $^{13}\text{C}\{^1\text{H}\}$  NMR ( $\text{C}_6\text{D}_6$ ):  $\delta$  135.71, 134.63, 130.12, 128.15, 27.11, 20.63. EI/MS [ $\text{M}/\text{Z}$ ]<sup>+</sup>: 819.9 [ $\text{NMo}(\text{OSiPh}_2\text{Bu})_3 - \text{CMe}_3$ ].

$\text{NMo}(\text{OCPh}_2\text{Me})_3$  (**17**). Solid 1,1-diphenylethanol (0.4588 g, 2.31 mmol, 3.2 equiv) was added to a stirring solution of **8** (0.1745 g, 0.721 mmol, 1.0 equiv) in THF (12 mL). The solution was stirred for 20 h; then the volatiles were removed *in vacuo*. The residue was dissolved in toluene (2 mL); then pentane (6 mL) was added to the solution, which was then cooled to  $-35\text{ }^{\circ}\text{C}$ . After 2 days, small colorless crystals of **17-NHMe**<sub>2</sub> formed on the sides of the crystallization vial, while several large amber blocks had grown at the bottom of the vial. The amber blocks were removed from the mother liquor and rinsed with pentane (1 mL); then they were redissolved in a solution of toluene (1.5 mL) and pentane (4 mL), which was then cooled to  $-35\text{ }^{\circ}\text{C}$ . Colorless clusters precipitated from the solution. The mother liquor was removed *via* pipet and the solid dried *in vacuo* to yield **17** (0.1062 g, 0.151 mmol, 21%) as white flakes.  $^1\text{H NMR}$  (400 MHz,  $\text{C}_6\text{D}_6$ ):  $\delta$  7.32–7.29 (m, 11H, ArH), 7.09–7.00 (m, 16H ArH), 2.03 (s, 9H,  $\text{CH}_3$ ).  $^{13}\text{C}\{^1\text{H}\}$  NMR ( $\text{C}_6\text{D}_6$ ):  $\delta$  148.54, 128.28, 127.19, 126.88, 87.74, 29.93. Anal. Calcd for  $\text{C}_{42}\text{H}_{39}\text{MoNO}_3$ : C, 71.89; H, 5.60; N, 2.00. Found: C, 71.93; H, 5.56; N, 1.84.

**Crystal Structure Determinations.** Complex **12**. Purple blocks of **12** were grown from an acetonitrile solution at  $-35\text{ }^{\circ}\text{C}$ . A crystal of dimensions  $0.38 \times 0.32 \times 0.23\text{ mm}$  was mounted on a Bruker SMART APEX CCD-based X-ray diffractometer equipped with a low temperature device and fine focus Mo-target X-ray tube ( $\lambda = 0.71073\text{ \AA}$ ) operated at 1500 W power (50 kV, 30 mA). The X-ray intensities were measured at 85(1) K; the detector was placed at a distance 5.055 cm from the crystal. A total of 5190 frames were collected with a scan width of  $0.5^\circ$  in  $\omega$  and  $0.45^\circ$  in  $\varphi$  with an exposure time of 15 s/frame. The integration of the data yielded a total of 190 801 reflections to a maximum  $2\theta$  value of  $60.22^\circ$ , of which 11 005 were independent and 10 231 were greater than  $2\sigma(I)$ . The final cell constants (Table 5) were based on the *xyz* centroids of 9793 reflections above  $10\sigma(I)$ . Analysis of the data showed negligible decay during data collection; the data were processed with SADABS and corrected for absorption. The structure was solved and refined with the Bruker SHELXTL (version 2008/4) software package, using the space group  $P2_1/n$  with  $Z = 4$  for the formula  $\text{C}_{38}\text{H}_{58}\text{N}_2\text{O}_3\text{Mo} \cdot \text{CH}_3\text{CN}$ . All non-hydrogen atoms were refined anisotropically with the hydrogen atoms placed in idealized positions except for the dimethylamino hydrogen, which was allowed to refine isotropically. Full matrix least-squares refinement based on  $F^2$  converged at  $R_1 = 0.0261$  and  $wR_2 = 0.0721$  [based on  $I > 2\sigma(I)$ ] and  $R_1 = 0.0286$  and  $wR_2 = 0.0747$  for all data.

Table 5. Crystallographic Parameters for **12** and **17-NHMe**<sub>2</sub>

	complex <b>12</b>	complex <b>17-NHMe</b> <sub>2</sub>
formula	$\text{C}_{40}\text{H}_{61}\text{MoN}_3\text{O}_3$	$\text{C}_{47.50}\text{H}_{50}\text{MoN}_2\text{O}_3$
fw	727.86	792.84
crystal system	monoclinic	triclinic
space group	$P2_1/n$	$P\bar{1}$
<i>a</i> (Å)	17.0283(9)	10.9987(16)
<i>b</i> (Å)	13.2624(7)	12.6721(18)
<i>c</i> (Å)	19.0848(10)	14.715(2)
$\alpha$ (deg)	90	87.778(2)
$\beta$ (deg)	114.780(1)	85.186(2)
$\gamma$ (deg)	90	78.835(2)
<i>V</i> (Å <sup>3</sup> )	3913.2(4)	2004.5(5)
<i>Z</i>	4	2
radiation (K $\alpha$ , Å)	0.71073	0.71073
<i>T</i> (K)	85(2)	85(2)
<i>D</i> <sub>calcd</sub> ( $\text{Mg m}^{-3}$ )	1.235	1.314
$\mu$ <sub>calcd</sub> ( $\text{mm}^{-1}$ )	0.374	0.371
<i>F</i> <sub>000</sub>	1552	830
<i>R</i> <sub>1</sub>	0.0261	0.0673
<i>wR</i> <sub>2</sub>	0.0747	0.1651
GO F	1.072	1.057

**Complex 17-NHMe**<sub>2</sub>. Colorless plates of **17-NHMe**<sub>2</sub> were grown from a toluene/pentane solution at  $-35\text{ }^{\circ}\text{C}$ . A crystal of dimensions  $0.26 \times 0.14 \times 0.12\text{ mm}$  was mounted on a Bruker SMART APEX CCD-based X-ray diffractometer equipped with a low temperature device and fine focus Mo-target X-ray tube ( $\lambda = 0.71073\text{ \AA}$ ) operated at 1500 W power (50 kV, 30 mA). The X-ray intensities were measured at 85(1) K; the detector was placed at a distance 5.055 cm from the crystal. A total of 3690 frames were collected with a scan width of  $0.5^\circ$  in  $\omega$  and  $0.45^\circ$  in  $\varphi$  with an exposure time of 30 s/frame. The integration of the data yielded a total of 40 336 reflections to a maximum  $2\theta$  value of  $53.08^\circ$ , of which 8251 were independent and 6223 were greater than  $2\sigma(I)$ . The final cell constants (Table 5) were based on the *xyz* centroids of 9312 reflections above  $10\sigma(I)$ . Analysis of the data showed negligible decay during data collection; the data were processed with SADABS and corrected for absorption. The structure was solved and refined with the Bruker SHELXTL (version 2008/3) software package, using the space group  $P\bar{1}$  with  $Z = 2$  for the formula  $\text{C}_{44}\text{H}_{46}\text{N}_2\text{O}_3\text{Mo} \cdot (\text{C}_6\text{H}_8)_{0.5}$ . All non-hydrogen atoms were refined anisotropically with the hydrogen atoms placed in idealized positions. The dimethylamine group is rotationally disordered over two equally occupied positions. The toluene solvate is located at an inversion center and is also disordered. Full matrix least-squares refinement based on  $F^2$  converged at  $R_1 = 0.0673$  and  $wR_2 = 0.1519$  [based on  $I > 2\sigma(I)$ ] and  $R_1 = 0.0948$  and  $wR_2 = 0.1651$  for all data.

## ■ ASSOCIATED CONTENT

**S Supporting Information.** Details of ACM and NACM reactions, additional NMR experiments, and crystallographic data for **12** and **17-NHMe**<sub>2</sub> in CIF format. This information is available free of charge via the Internet at <http://pubs.acs.org>.

## ■ AUTHOR INFORMATION

### Corresponding Author

\*E-mail: [mjjohnson@anl.gov](mailto:mjjohnson@anl.gov).

## Present Addresses

<sup>5</sup>Chemical and Materials Sciences Division, Pacific Northwest National Laboratory, Richland, Washington 99352, United States.

## ACKNOWLEDGMENT

This material is based upon work supported by the National Science Foundation under Grant No. CHE-0449459 and by the Department of Energy, Office of Basic Energy Sciences, Chemical Sciences program. Argonne National Laboratory is a U.S. Department of Energy, Office of Science laboratory operated under Contract No. DE-AC02-06CH11357. We also thank the University of Michigan for financial support.

## REFERENCES

- (1) (a) Grubbs, R. H. *Handbook of Metathesis*; Wiley-VCH: Weinheim, Germany, 2003; Vol. 2 - Applications in Organic Synthesis, p 510. (b) Grubbs, R. H. *Handbook of Metathesis*; Wiley-VCH: Weinheim, Germany, 2003; Vol. 3 - Applications in Polymer Synthesis, p 442. (c) Schrock, R. R.; Czekelius, C. *Adv. Synth. Catal.* **2007**, *349*, 55–77.
- (2) (a) Furstner, A.; Davies, P. W. *Chem. Commun.* **2005**, 2307–2320. (b) Furstner, A.; Radkowski, K.; Grabowski, J.; Wirtz, C.; Mynott, R. J. *Org. Chem.* **2000**, *65*, 8758–8762.
- (3) (a) Bunz, U. H. F.; Kloppenburg, L. *Angew. Chem., Int. Ed.* **1999**, *38*, 478–481. (b) Brizius, G.; Pschirer, N. G.; Steffen, W.; Stitzer, K.; zur Loye, H. C.; Bunz, U. H. F. *J. Am. Chem. Soc.* **2000**, *122*, 12435–12440. (c) Ge, P. H.; Fu, W.; Herrmann, W. A.; Herdtweck, E.; Campana, C.; Adams, R. D.; Bunz, U. H. F. *Angew. Chem., Int. Ed.* **2000**, *39*, 3607–3610.
- (4) (a) Zhang, W.; Moore, J. S. *Adv. Synth. Catal.* **2007**, *349*, 93–120. (b) Zhang, W.; Moore, J. S. *Angew. Chem., Int. Ed.* **2006**, *45*, 4416–4439. (c) Cho, H. M.; Weissman, H.; Wilson, S. R.; Moore, J. S. *J. Am. Chem. Soc.* **2006**, *128*, 14742–14743. (d) Zhang, W.; Moore, J. S. *J. Am. Chem. Soc.* **2005**, *127*, 11863–1870. (e) Zhang, W.; Moore, J. S. *J. Am. Chem. Soc.* **2004**, *126*, 12796–12796.
- (5) Goodson, F. E.; Wallow, T. I.; Novak, B. M. *J. Am. Chem. Soc.* **1997**, *119*, 12441–12453.
- (6) Naddo, T.; Che, Y. K.; Zhang, W.; Balakrishnan, K.; Yang, X. M.; Yen, M.; Zhao, J. C.; Moore, J. S.; Zang, L. J. *J. Am. Chem. Soc.* **2007**, *129*, 6978–6979.
- (7) Furstner, A.; Mathes, C.; Lehmann, C. W. *Chem.—Eur. J.* **2001**, *7*, 5299–5317.
- (8) (a) North, M. In *Comprehensive Organic Functional Group Transformations II*, 1st ed.; Katritzky, A. R., Taylor, R. J. K., Eds.; Elsevier: Amsterdam, 2005; Vol. 3, p 621. (b) Tyrrell, E. In *Comprehensive Organic Functional Group Transformations II*, 1st ed.; Katritzky, A. R., Taylor, R. J. K., Eds.; Elsevier: Amsterdam, 2005; Vol. 1, p 1083.
- (9) Geyer, A. M.; Gdula, R. L.; Wiedner, E. S.; Johnson, M. J. A. *J. Am. Chem. Soc.* **2007**, *129*, 3800–3801.
- (10) Geyer, A. M.; Wiedner, E. S.; Gary, J. B.; Gdula, R. L.; Kuhlmann, N. C.; Johnson, M. J. A.; Dunietz, B. D.; Kampf, J. W. *J. Am. Chem. Soc.* **2008**, *130*, 8984–8999.
- (11) Gdula, R. L.; Johnson, M. J. A. *J. Am. Chem. Soc.* **2006**, *128*, 9614–9615.
- (12) Bindl, M.; Stade, R.; Heilmann, E. K.; Picot, A.; Goddard, R.; Furstner, A. *J. Am. Chem. Soc.* **2009**, *131*, 9468–9470.
- (13) Gdula, R. L. Ph.D. Dissertation, University of Michigan, Ann Arbor, MI, 2006.
- (14) Geyer, A. M. Ph.D. Dissertation, University of Michigan, Ann Arbor, MI, 2009.
- (15) Heppekaussen, J.; Stade, R.; Goddard, R.; Furstner, A. *J. Am. Chem. Soc.* **2010**, *132*, 11045–11057.
- (16) Schrock, R. R. *Acc. Chem. Res.* **1986**, *19*, 342–348.
- (17) (a) Churchill, M. R.; Ziller, J. W.; Freudenberger, J. H.; Schrock, R. R. *Organometallics* **1984**, *3*, 1554–1562. (b) Freudenberger, J. H.; Schrock, R. R.; Churchill, M. R.; Rheingold, A. L.; Ziller, J. W. *Organometallics* **1984**, *3*, 1563–1573.
- (18) McCullough, L. G.; Schrock, R. R. *J. Am. Chem. Soc.* **1984**, *106*, 4067–4068.
- (19) Zhu, J.; Jia, G.; Lin, Z. *Organometallics* **2006**, *25*, 1812–1819.
- (20) McCullough, L. G.; Schrock, R. R.; Dewan, J. C.; Murdzek, J. C. *J. Am. Chem. Soc.* **1985**, *107*, 5987–5998.
- (21) Gdula, R. L.; Johnson, M. J. A.; Ockwig, N. W. *Inorg. Chem.* **2005**, *44*, 9140–9142.
- (22) (a) Chisholm, M. H.; Delbridge, E. E.; Kidwell, A. R.; Quinlan, K. B. *Chem. Commun.* **2003**, 126–127. (b) Burroughs, B. A.; Bursten, B. E.; Chen, S.; Chisholm, M. H.; Kidwell, A. R. *Inorg. Chem.* **2008**, *47*, 5377–5385.
- (23) Nugent, W. A.; Mayer, J. M. *Metal-Ligand Multiple Bonds*; John Wiley & Sons: New York, 1988; p 26–29.
- (24) Mayer, J. M. *Polyhedron* **1995**, *14*, 3273–3292.
- (25) Schrock, R. R. *Polyhedron* **1995**, *14*, 3177–3195.
- (26) Olmstead, W. N.; Margolin, Z.; Bordwell, F. G. *J. Org. Chem.* **1984**, *49*, 1424–1427.
- (27) Ballinger, P.; Long, F. A. *J. Am. Chem. Soc.* **1960**, *82*, 795–798.
- (28) Bordwell, F. G. *Acc. Chem. Res.* **1988**, *21*, 456–463.
- (29) Bordwell, F. G.; McCallum, R. J.; Olmstead, W. N. *J. Org. Chem.* **1984**, *49*, 1424–1427.
- (30) Steward, O. W.; Fussaro, D. R. *J. Organomet. Chem.* **1977**, *129*, C28–C32.
- (31) Chan, D. M. T.; Chisholm, M. H.; Folting, K.; Huffman, J. C.; Marchant, N. S. *Inorg. Chem.* **1986**, *25*, 4170–4174.
- (32) Johnson, M. J. A.; Lee, P. M.; Odom, A. L.; Davis, W. M.; Cummins, C. C. *Angew. Chem., Int. Ed. Engl.* **1997**, *36*, 87–91.
- (33) Tsai, Y. C.; Johnson, M. J. A.; Mindiola, D. J.; Cummins, C. C.; Klooster, W. T.; Koetzle, T. F. *J. Am. Chem. Soc.* **1999**, *121*, 10426–10427.
- (34) Laplaza, C. E.; Johnson, M. J. A.; Peters, J. C.; Odom, A. L.; Kim, E.; Cummins, C. C.; George, G. N.; Pickering, I. J. *J. Am. Chem. Soc.* **1996**, *118*, 8623–8638.
- (35) Addison, A. W.; Rao, T. N.; Reedy, K. J.; van Rijn, J.; Verschoor, G. C. *J. Chem. Soc., Dalton Trans.* **1984**, 1349–1356.
- (36) An analysis of the Cambridge Crystallographic Database (August 2010) revealed 60 structures with a Mo nitrido ligand (both terminal and oligomeric), with an average Mo–N triple bond length of 1.662(33) Å.
- (37) Sancho, J.; Schrock, R. R. *J. Mol. Catal.* **1982**, *15*, 75.
- (38) Finke, A. D.; Moore, J. S. *Chem. Commun.* **2010**, 46, 7939–7941.
- (39) Pangborn, A. B.; Giardello, M. A.; Grubbs, R. H.; Rosen, R. K.; Timmers, F. J. *Organometallics* **1996**, *15*, 1518–1520.
- (40) Mullen, D. G.; Barany, G. *J. Org. Chem.* **1988**, *53*, 5240–5248.
- (41) Bradley, D. C.; Thomas, I. M. *J. Chem. Soc.* **1960**, 3857–3861.